High Resolution Holoscopy

Gesa Lilith Franke[1,2], Dierck Hillmann[2,3], Thorsten Claußen[3], Christian Lührs[3], Peter Koch[3], Gereon Hüttmann[1]

[1]Institute of Biomedical Optics, University of Lübeck, Germany
[2]Medical Laser Center Lübeck, Germany
[3]Thorlabs GmbH, Germany

ABSTRACT

Holoscopy is a new imaging approach combining Digital Holography and Full-field Fourier-domain Optical Coherence Tomography. The interference pattern between the light scattered by a sample and a defined reference wave is recorded digitally. By numerical processing of the recorded interference pattern, the back-scattering field of the sample is reconstructed with a diffraction limited lateral resolution over the whole measurement depth since numerical refocusing overcomes the limitation of the focal depth. We present two setup configurations – a low resolution setup based on a Michelson interferometer and a high resolution setup based on a Mach-Zehnder interferometer. Successful measurements were demonstrated with a numerical aperture (NA) of 0.05 and 0.14, respectively and will be presented. Additionally, the effects of filtering spatial frequencies in terms of separating sample signals from artifacts caused by setup reflections is discussed and its improvement on the image quality is shown.

Keywords: optical coherence tomography, digital holography, holoscopy, optical coherence microscopy, tomography, microscopy

1. INTRODUCTION

In Fourier-domain Optical Coherence Tomography (FD-OCT) the lateral and axial resolution are decoupled. While the constant axial resolution is defined by the center wavelength and the spectral width of the light source, the lateral resolution is defined by the optical layout which images the backscattered light on the detector. According to Gaussian optics the lateral resolution in the focal plane increases with NA while the imaging depth (described by the Rayleigh length) decreases due to degradation of the resolution. Additionally, in scanning FD-OCT photons from outside the Rayleigh length are suppressed due to the confocal gating. This can be nicely seen when imaging point scatterers – particles with a size below the lateral resolution. In Fig. 1a a polyurethane resin doped red iron oxide particles (particle size: $300 - 800\,\mathrm{nm}$)[1] was imaged with a scanning FD-OCT device. With the Full-field (FF) FD-OCT approach[2,3] photons from all depths over the measurement range can be detected but the degraded lateral resolution causes blurred images outside the focal plane (Fig. 1b). Holoscopy is a new imaging approach combining Digital Holography (DH) and FF-FD-OCT.[4]
By applying virtual refocussing mechanisms as in DH a diffraction limited depth-independent lateral resolution is provided over the whole penetration depth (Fig. 1c). Comparable to FF-OCT photons are detected from all depths but there is no Rayleigh length restriction of the imaging depth. For a lens-less setup the remaining restrictions are the signal roll-off well known in FD-OCT caused by the limited coherence length of the laser and the penetration depth of the incident light. This advantage of Holoscopy can be clearly seen at quite low NA (Fig. 1) but becomes even more significant when going to higher lateral resolutions. In most other optical imaging techniques z-scanning is inevitable for measuring a high resolution tomographic volume of a sample.

Further author information:
G.F.: E-mail: franke@bmo.uni-luebeck.de, Telephone: +49 (0) 451 500 6510
D.H.: E-mail: hillmann@mll.uni-luebeck.de, Telephone: +49 (0) 451 500 6510
P.K.: E-mail: pkoch@thorlabs.com, Telephone: +49 (0) 451 290 3370
G.H. E-mail: huettmann@bmo.uni-luebeck.de, Telephone: +49 (0) 451 500 6530

Optical Coherence Tomography and Coherence Domain Optical Methods in Biomedicine XVI,
edited by Joseph A. Izatt, James G. Fujimoto, Valery V. Tuchin, Proc. of SPIE Vol. 8213, 821324

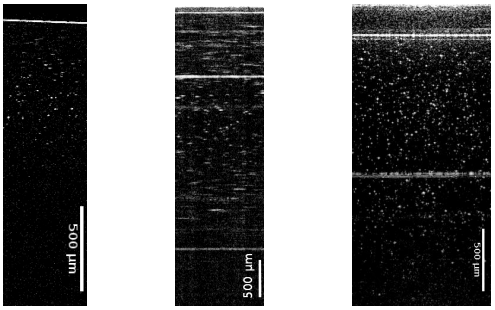

(a) (b) (c)

Figure 1: B-scans of a phantom with scattering particles acting as point scatterers imaged with a numerical aperture (NA) of 0.05. a) Scanning FD-OCT showing the limited imaging depth due to the confocal gating and Gaussian optics. The imaging quality degrades outside the focus with respect to resolution and sensitivity, respectively. b) Full-field FD-OCT shows higher sensitivity outside the focus region due to the lack of a confocal gating. Nevertheless, the resolution still degrades outside the focus. c) Holoscopy shows constant resolution and sensitivity over the complete measurement depth.

2. SETUP CONFIGURATIONS FOR LOW AND HIGH RESOLUTION MEASUREMENTS

Holoscopy measurements can be performed with holographic setups for reflective samples. In most cases a holographic setup consists of a interferometer with a monochromatic long coherent light source. With an area detector the amplitude and phase of the light field as backscattered by the sample is recorded, which is encoded in the fringe pattern of the interference signal between sample and reference light. Imaging optics does not have to be implemented but can be used for magnification.[5,6] In Holoscopy the monochromatic light source is replaced by a tunable laser. Setups can be implemented using for example Michelson or Mach-Zehnder type interferometer configurations where the sample is positioned in one arm. Schematic setups for both configurations can be seen in Fig. 2. The Michelson setup (Fig. 2a) consists of a beam splitter for splitting the light to illuminate sample and reference mirror and superimposing the wave fields of the backscattered and reflected light of sample and reference arm, respectively. To provide optimum sampling of the spatial frequencies of the interference pattern and thus to achieve maximum NA the reference beam is shaped by using a spherical mirror. The interfering wave fields of sample and reference arm are detected by an area camera. This setup was implemented with the following components. The reference arm was assembled with a convex mirror with a focal length of $f = -10.34\,\mathrm{mm}$. The tunable laser (BroadSweeper BS-840-01, Superlum) has a center wavelength of $\lambda_0 = 848.5\,\mathrm{nm}$ and a spectral width of $\Delta\lambda = 50\,\mathrm{nm}$ corresponding to $14\,\mu\mathrm{m}$ axial resolution after Hann windowing of the spectrum. For *ex-vivo* measurements a monochromatic CMOS camera (Mikrotron EoSens MC3010) with $1536 \times 1536\,\mathrm{pixel}$ and a pixel size of $\Delta x = 8\,\mu\mathrm{m}$ was used as the detector. However, only a subregion of $1024 \times 1024\,\mathrm{pixel}$ was used. This resulted in a lateral resolution of $2w_0 = 11\,\mu\mathrm{m}$ and a Rayleigh length of $2z_R = 200\,\mu\mathrm{m}$. The imaging speed was 630 frames/s. For *in-vivo* measurements a high-speed CMOS camera (Photron Fastcam SA5) with $1024 \times 1024\,\mathrm{pixel}$ and a pixel size of $\Delta x = 20\,\mu\mathrm{m}$ was used as the detector corresponding to a lateral resolution of $2w_0 = 8\,\mu\mathrm{m}$ and a Rayleigh length of $2z_R = 100\,\mu\mathrm{m}$. The imaging speed was 7000 frames/s. The NA and thus the lateral resolution of this setup were given by the distance of the sample to the camera and the NA increased when the sample was positioned closer to the camera plane. However, when putting the sample closer to the camera spatial frequencies, which encode the lateral structures, also increase. If the sample was positioned too close to the camera the spatial fringes could no longer be resolved by the camera thus limiting the achievable lateral resolution. Higher lateral resolution can be achieved with the setup shown in Fig. 2b. In this Mach-Zehnder based setup the sample is illuminated with a collimated beam via an achromatic lens and a microscope objective. The backscattered light field of the sample is magnified by the microscope objective before reaching the camera. The reference beam is a collimated beam which is implemented off-axis, i. e. which incidents with an angle onto the camera. As commonly used in DH this enables the separation of the image from autocorrelated and DC parts as well as the complex conjugate image[5] and thus reduces artifacts due to reflexes from within the setup. The lateral resolution of this setup is determined by the NA of the microscope objective, as long

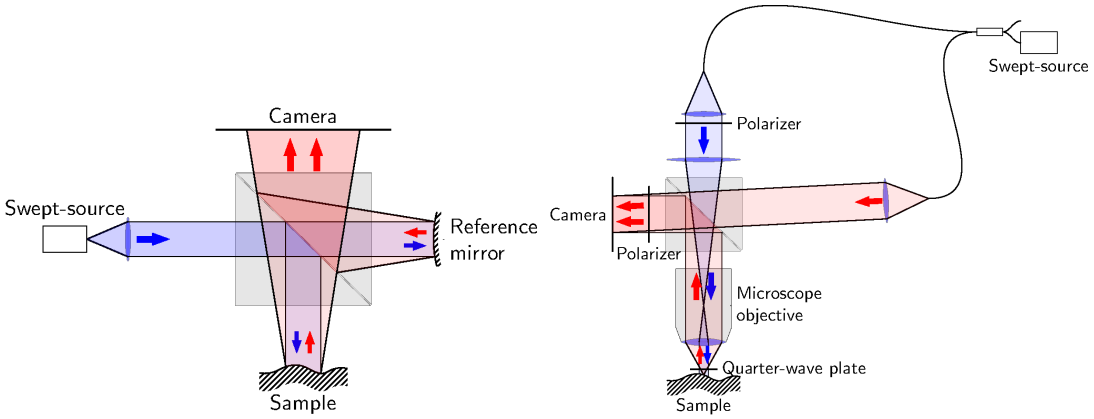

Figure 2: Setups that were used for holoscopic imaging. a) Low resolution setup, a lens-less design based on a Michelson interferometer. b) Mach-Zehnder configuration for high resolution measurements, where a microscope objective is used to magnify the sample wave field.

as the enlarged sample wave field can be sampled correctly. The setup was implemented with the following components. In the sample arm a 2.15 mm beam was reshaped to a 1.23 mm beam via an achromate with a focal length of $f = 75$ mm and a microscope objective with an NA of 0.14 (5× Mitotuyo Plan Apo NIR Infinity-Corrected Objective, $f = 40$ mm). This NA results in a lateral resolution of $2w_0 = 3.8\,\mu$m and a Rayleigh length of $2z_R = 27\,\mu$m. The diameter of the collimated reference wave was 16 mm which was superimposed with the backscattered light of the sample on the camera (Basler Ace, 2048 × 2048 pixel with an acquisition speed of 127 frames/s and a pixel size of $\Delta x = 5.5\,\mu$m). As light source a tunable laser (BroadSweeper BS 840-HR, Superlum) with a center wavelength of $\lambda_0 = 841$ nm and a spectral width of $\Delta\lambda = 82$ nm was implemented corresponding to an axial resolution of 8.6 μm after Hann windowing of the spectrum. To additionally suppress background noise on the camera caused by reflections from within the setup the sample arm was assembled with two polarization filters – one right after the collimator and the other one in front of the camera – and a quarter wave plate in front of the sample. With this configuration the light reflected from within the setup is blocked while the light scattered by the sample is detected without attenuation.

RECONSTRUCTION

To obtain diffraction limited lateral resolution over the whole imaging depth Holoscopy combines elements from FD-OCT and DH. In DH the light field of a reflecting sample is detected by recording its interference pattern with a known reference wave with an area detector. The sample information is encoded in the fringe pattern of the interference signal – also called hologram. By applying a two-dimensional Fourier transform the sample light field is decoded in the Fourier plane. When the reference beam is positioned off-axis to the sample beam a spatial carrier frequency separates the sample light field from the DC parts of the hologram and its complex conjugate image. By applying a suitable filter the cross-correlation image is selected and after an inverse Fourier transform a complex hologram without DC parts and without conjugate image is achieved. By multiplication with a reconstruction wave and subsequent numerical back propagation of the sample light field into a plane inside the sample a sharp image of the chosen layer is obtained. The propagation can for example be performed using the angular spectrum approach, where each hologram is decomposed into plane waves and each plane wave is then propagated independently. Finally the plane waves are re-superimposed to give the propagated data.[5] This reconstruction algorithm works well for three-dimensional surfaces and very low scattering samples. If holographic reconstruction is applied to scattering samples, the sample information is disturbed since the light fields of all scatterers superimpose (Fig. 3a). This results in an overlay of sharp and blurred images and thus a loss of the sample information. In Holoscopy this reconstruction process is applied to each hologram that was acquired during the sweep, where the respective wavelength is used for reconstruction and all wave fields are

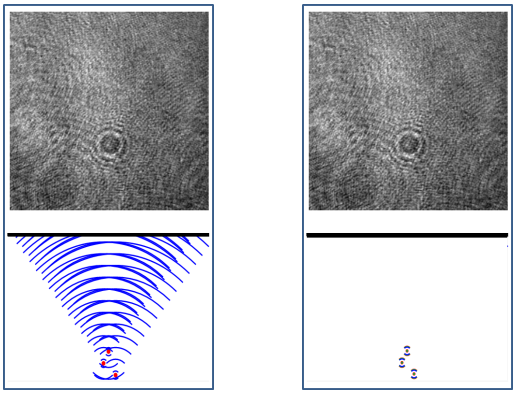

(a) (b)

Figure 3: a) Reconstruction limitation of holography for scattering samples – refocusing in one layer results in an overlay of sharp and out-of-focus images. b) Applying the Holoscopy image reconstruction algorithm, scattering structures can be distinguished over depth.

propagated to the same layer within the sample. Finally, a one-dimensional Fourier transform along the wave number axis – with suitable re-sampling if the sweep is non-linear in k – gives the depth information. As the original raw data is still available the procedure can be repeated with a different reconstruction layer and thus a different numerical focus. By stitching together reconstructions for all layers a constant, diffraction limited resolution can be achieved.

3. RESULTS

We demonstrated successful measurements with both introduced setups providing a low resolution imaging modality for high-speed measurements and a high resolution configuration for resolving cellular structures. Using the Michelson type setup and a high-speed camera we performed *in-vivo* measurements of a finger tip (Fig. 4). Measurements were performed with 7000 fps for a data volume of $1024 \times 1024 \times 512$ voxel. This corresponds to an imaging speed of $3.5 \cdot 10^6$ voxel/s with an image quality comparable to FF-FD-OCT measurements. The simple setup design without optical components results in images without significant artifacts. Remaining artifacts could be assigned to a protective glass window in front of the camera sensor. However, the high resolution setup

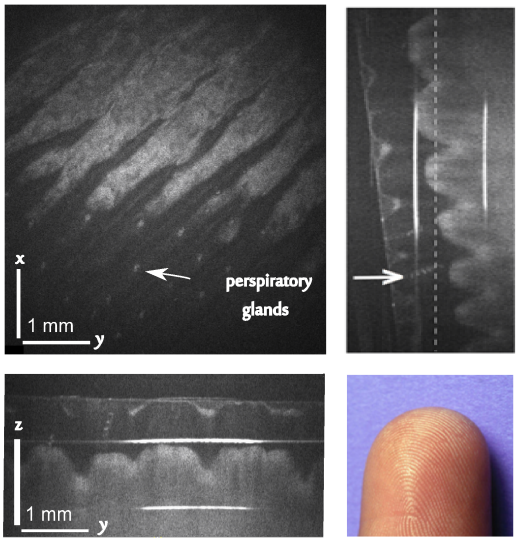

Figure 4: *In-vivo* measurement of a finger tip showing the possibility to provide high-speed acquisition.

with an implemented microscope objective results in images suffering from severe artifacts due to reflections from within the setup when having an on-axis illumination as in the Michelson-based setup. Those artifacts can be significantly reduced when implementing an off-axis illumination. We compared holoscopic reconstructions for on-axis and off-axis setups to show the suppression of DC terms and autocorrelation noise as shown in Fig. 5. It can be seen that image, conjugate image and DC parts overlap in the on-axis geometry (Fig. 5c) which results in a bright central part of the reconstructed tomogram and reduced imaging quality (Fig. 5b) due to reflexes induced by setup components. By using the off-axis geometry the images can clearly be separated as seen in the Fourier plane (Fig. 5c). The resulting B-scan shows significantly reduced imaging artifacts (Fig. 5d). To compare both setups introduced in the previous section measurements of onions and grapes were performed with both setups. Fig. 6 shows the resulting en-face images. All images clearly demonstrate the capabilities of Holoscopy to measure three-dimensional tomograms. However, the Michelson type setup with its limited NA fails to resolve cell structures of the onion (Fig. 6a) and is also not able to show smaller structures in the grape (Fig. 6b). However, using the Mach-Zehnder type setup using a microscope objective with an NA of 0.14, cell structures of the onion and smaller structures within the grape are clearly visible (Fig. 6c and Fig. 6d, respectively).

4. DISCUSSION AND OUTLOOK

We demonstrated the capabilities of Holoscopy as a new imaging technique overcoming several shortcomings of Fourier-domain OCT. Holoscopy is capable of providing high quality images with a high resolution and sensitivity that is constant over the complete measurement depth. Its principle promises to provide microscopic resolution in three dimensions, with high acquisition speeds enabling *in-vivo* measurements. Therefore, we will increase the NA of the high resolution setup from 0.14 to 0.4, corresponding to a lateral resolution of 1.3 μm. Accordingly the axial resolution will be increased as well to obtain an almost isotropic resolution. This will be achieved by tuning a Ti:sapphire laser over its spectral range ($\sim$ 300 nm spectral width). Furthermore we will try and evaluate improvements to the setup and to the reconstruction algorithms to reduce image artifacts and increase

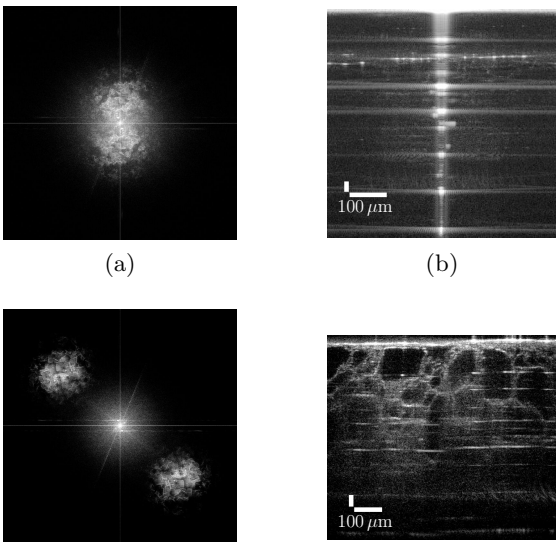

(a) (b)

(c) (d)

Figure 5: a) Fourier plane of one hologram of a grape that was captured using on-axis illumination. Image, conjugate image, DC and autocorrelated parts can not be distinguished. b) B-scan of a grape, obtained by holocopic reconstruction of a data set recorded with on-axis illumination. Artefacts are seen in the center of the image and clearly disturb the image. Imaging quality is significantly reduced. c) Fourier plane of one hologram of a grape that was captured using off-axis illumination. Image, conjugate image, DC and autocorrelated parts can now clearly be distinguished. d) B-scan of a grape, obtained by holocopy reconstruction of a data set recorded with off-axis illumination. Although remaining artifacts are visible, imaging quality is clearly increased compared to (b).

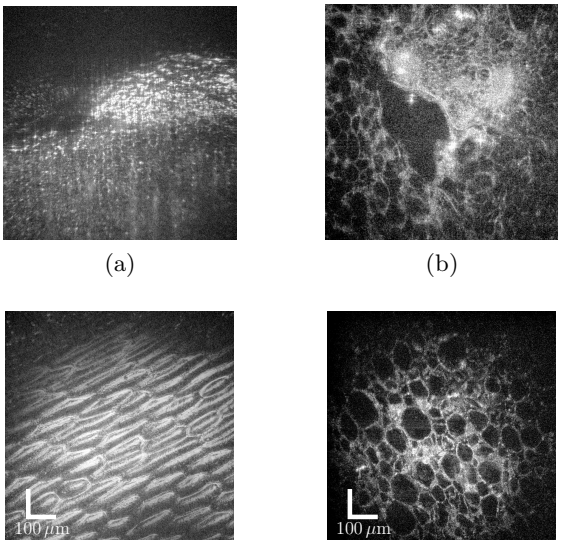

(a) (b)

(c) (d)

Figure 6: En-face images acquired using a Michelson type setup with a low NA of 0.05 of an onion (a) and a grape (b). Cell structures of the onion and smaller structures of the grape are not visible. In corresponding images acquired using a Mach-Zehnder type setup with an NA of 0.14, cell structures are now clearly visible in the onion (c) and also smaller structures of the grape could be resolved (d).

imaging quality. Finally a greater variety of samples will be investigated to provide more information about the capabilities and limitations of Holoscopy.

REFERENCES

[1] Woolliams, P. D., Ferguson, R. A., Hart, C., Grimwood, A., and Tomlins, P. H., "Spatially deconvolved optical coherence tomography," *Appl Opt* **49**, 2014–21 (Apr 10 2010).

[2] Považay, B., Unterhuber, A., Hermann, B., Sattmann, H., Arthaber, H., and Drexler, W., "Full-field time-encoded frequency-domain optical coherence tomography," *Opt. Express* **14**(17), 7661–7669 (2006).

[3] Bonin, T., Franke, G., Hagen-Eggert, M., Koch, P., and Hüttmann, G., "In vivo fourier-domain full-field oct of the human retina with 1.5 million a-lines/s," *Opt. Lett.* **35**(20), 3432–3434 (2010).

[4] Hillmann, D., Lührs, C., Bonin, T., Koch, P., and Hüttmann, G., "Holoscopy—holographic optical coherence tomography," *Opt. Lett.* **36**, 2390–2392 (Jul 2011).

[5] Kim, M. K., "Principles and techniques of digital holographic microscopy," *SPIE Reviews* **1**(1), 018005 (2010).

[6] Schnars, U. and Jueptner, W., [*Digital holography*], Springer (2005).